The International Journal of Advanced Manufacturing Technology (2018) 97:1431–1444
https://doi.org/10.1007/s00170-018-2047-1

ORIGINAL ARTICLE

Experimental study on the fabrication method of diamond ultra-small micro-grinding tool

J. Cheng [1] · J. Wu [1]

Received: 19 September 2017 / Accepted: 17 April 2018 / Published online: 26 April 2018

Abstract
This paper mainly focuses on the fabrication process of diamond ultra-small micro-grinding tool, on which a novel fabrication method is presented and applied. Models for tool substrate (tungsten carbide) machining and tool electroplating in this new method are built, during which the inclined angle (θ) and the electroplating thickness value (δ_{tp}) of point discharge effect are considered. By this method, a series of ultra-small micro-grinding tools, whose diameters are from 6 to 120 μm, are successfully fabricated. The deposition velocity of electroplating layer caused by point discharge effect (v_{tp}) is found to be influenced mainly by cathode-current density (D_k). The critical D_k value for the occurrence of point effect is delayed to above 0.6 A/dm^2 from conventional of about 0.3 A/dm^2, almost tripled than the traditional way. The effect caused by tool diameter (d_0) to electroplating thickness (δ_{mt}) is found to be irregular based on a comparison of the equivalent thickness (δ_{me}). By conducting a group of micro-grinding experiments on single crystal silicon, the brittle-ductile transition is observed. Above all, an ultra-small micro-grinding tool, whose diameter (d_s) is less than 20 μm and the length-to-diameter ratio (L/D) is larger than 1:50, is fabricated, and this is the most extreme length-to-diameter ratio in this scale. The ultra-small micro-grinding tool manufactured by this method is successfully verified by experiments. This study is quite meaningful for promoting the development of precision micro-machining industry.

Keywords Ultra-small micro-grinding tool · Tungsten carbide · Fabrication process · Point discharge effect

1 Introduction

Novel diamond micro-tools, especially diamond ultra-small micro-grinding tools, due to its high potential business value and the rapid increasing demand in optical industry, semiconductor industry, military industry, and so on, have absorbed a rising attention from researchers to the application and the most important development of tool fabrication [1]. Especially in the requirement from fuel injection nozzle for automobiles and biotechnology micro-products, the micro-machining technology plays a more vital role [2]. For mechanical micro-machining, more advanced miniature micro-grinding tool and micro-milling tool have been developed, and some high-precision 2D and 3D products have been successfully produced by using them [3].

There are several technologies for fabrication of diamond micro-grinding tool. Smith and Axinte innovatively designed a kind of diamond micro-grinding tool, which combined YAG laser and grain electroplating technology, and finally achieved good machining results on difficult-to-cut material [4]. A novel micro-core drill made from solid PCD using defined edge geometries also was developed and showed significant results in the experiments [1]. Precision end-face grinding is also an efficient choice for the substrate machining, and the efforts devoted to micro-machining and micro-tool fabrication technology have made a huge improvement in the past 20 years.

Other fabrication methods such as wire electrical discharge grinding (WEDG) and micro-electrochemical discharge machining (EDM) are also employed for making the tool substrate, then the grains are coated to the tool surface by electroplating or by other methods. Morgan et al. fabricated micro-tools such as miniature end mill, drill, or abrasive wheel by micro-EDM [5]. Chen et al. designed a funnel mold to improve the grain dispersing performance, the diameter of metal substrate was firstly cut down to 50 μm by using WEDG [6], and the 0–2-μm-sized grains are *plated* on the

✉ J. Cheng
Jcheng@mail.neu.edu.cn

[1] Advanced Manufacturing Institute, Northeastern University, P.O. Box 319, Shenyang, People's Republic of China 110004

surface of the substrate by composite electroforming. The fabricated micro-tools are successfully used for grinding the precision ceramic component. Chen et al. fabricated an innovative bench-top drill, which combines micro-EDM with grinding and drilling, to fabricate micro-holes in optical grade glass [7], and the achieved ductile grinding regime in experiments shows a good attribute of this micro-tool. Cheng et al. developed a new micro-drill grinding tool for precision micro-drilling of hard-brittle materials, such as alumina ceramic and soda-lime glass [8], and analyzed the material removal mechanism of micro-drill grinding.

For getting a better processing performance, micro-grinding is attracting more research interests since it is an important method for precision micro-machining of hard-brittle materials [9]. Denkena et al. discussed the influence of micro-geometry on the surface quality in micro-grinding and noted that the usage of ultra-small sonic-assisted grinding is a potential technique to minimize this influence [10]. Feng et al. investigated the wear process in micro-grinding of ceramic, and the relation between material removal volume and tool wear is investigated based on experimental results [11]. Park and Liang proposed a model to predict micro-grinding force of single crystal silicon, of which the size of crystal was considered [12]. Lee and Lee proposed a method to characterize a micro-grinding process under compressed chilly air condition [13], and experimental results show the effectiveness of compressed chilly air and its ability to improve tool life due to the decreased grinding forces in the micro-grinding process. Cheng et al. evaluated single crystal sapphire with three different surface orientations in micro-slot grinding and provided fundamental knowledge of the effect that crystalline anisotropy caused to the micro-slot grinding force [14]. Some other researchers also had made brilliant work in micro-grinding tool fabrication, such as Chen and Lai [15] who built several micro-scale grinding tools by WEDG, electroforming, electrochemical co-deposition, and RWEDM. Aurich et al. [16] achieved the most precise surface by micro-grinding (10 nm roughness) and fabricated a series of micro-grinding tools (diameter between 13 and 100 μm). Ohmori et al. [17] investigated the microscopic grinding effect in the fabrication process of ultra-fine micro-tool substrate. And, in the micro-scale, the grit temperature and stress distribution which are significant to the grinding tool fabrication also have been deeply investigated [18, 19].

Considering all of those above, it is clear that there exist difficulties in the fabrication and efficiency of

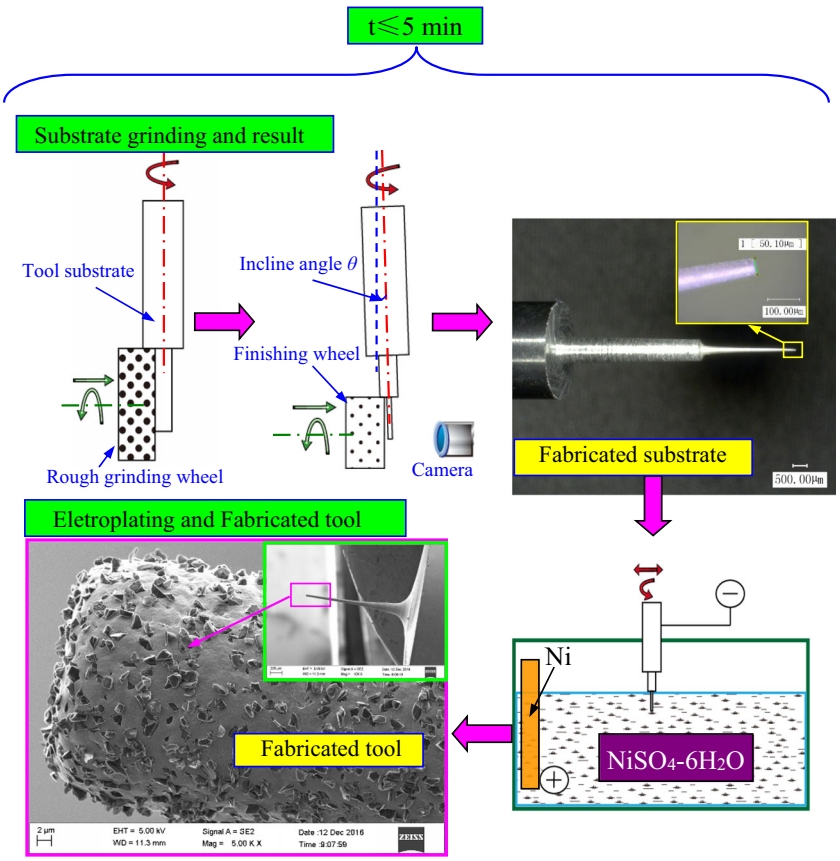

Fig. 1 Fabrication procedure for the ultra-small micro-grinding tool

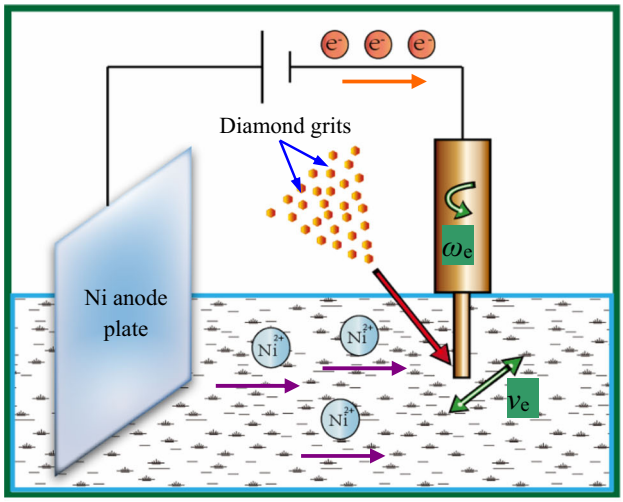

(a) Electroplating process for ultra small micro-tool

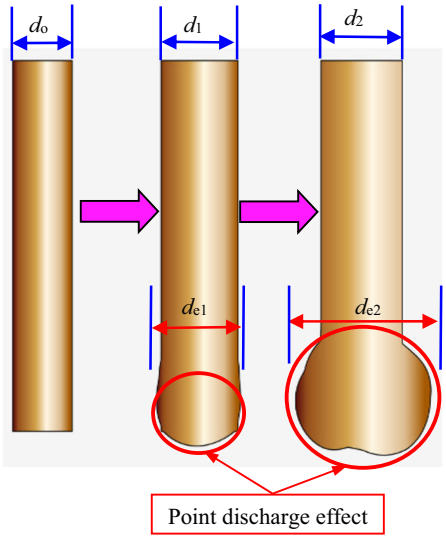

(b) Point discharge effect

Fig. 2 Electroplating process and effect in the fabrication of ultra-small micro-grinding tool. **a** Electroplating process for the ultra-small micro-tool. **b** Point discharge effect

diamond micro-grinding tool, especially for the ultra-small micro-grinding tool. In order to significantly improve the efficiency of micro-grinding tool making, especially the ultra-small micro-grinding tool, this study presents a novel method for micro-grinding tool fabrication. The equipment for this new method is developed by this study. The effectiveness and efficiency of this method have been proved by a series of fabricated diamond micro-tools and their successfully experimental results. The method of this study has advantages such as high machining efficiency and low processing difficulty over existing fabrication methods.

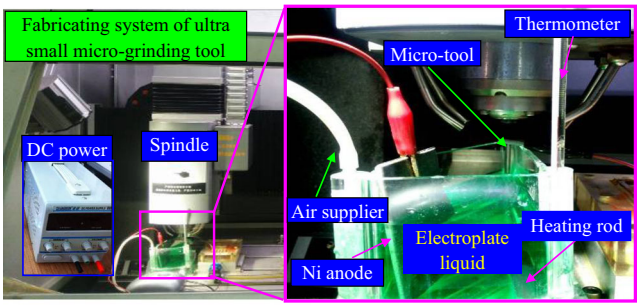

(a) Fabricating electroplating apparatus of ultra small grinding tool

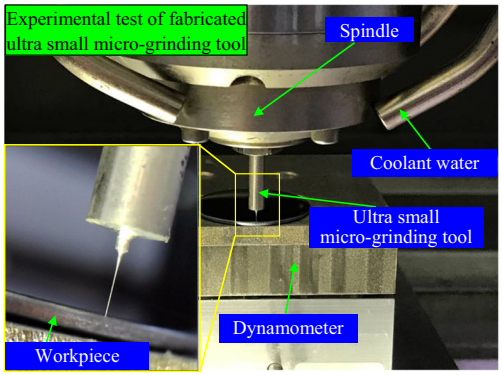

(b) Experimental validation with fabricated ultra small micro-grinding tool

Fig. 3 Fabricating and validating system of ultra-small micro-grinding tool. **a** Fabricating electroplating apparatus of ultra-small grinding tool. **b** Experimental validation with fabricated ultra-small micro-grinding tool

2 Development of fabrication method

2.1 Design of procedure

In order to improve the fabrication process of diamond ultra-small micro-grinding tool, this study proposes a new fabrication method, which is shown in Fig. 1. The fabrication procedures of this new method has been proposed and successfully carried out, and the substrate machining is an important step in these methods.

In traditional process, the tool substrate is fabricated by surface grinding: first, grinding to 100~200 μm diameter from 500 μm, and second, machining to less than 50 μm by precision grinding, which is time consuming. And, some consequent additional shape optimization processes such as μEDM also costs a lot of time, almost above 15 min for single tool fabrication. WEDG is another widely used method for micro-tool substrate machining, and this method has a wide range usage for micro-tool fabrication. The shortage of WEDG is that it is difficult to achieve a good substrate surface for micro-tools in ultra-small scale (5 to 50 μm), and the production efficiency is low.

As shown in Fig. 1, the procedure of this new method is different from a traditional grinding method adopted in the micro-tool making process. Firstly, the substrate of micro-tool

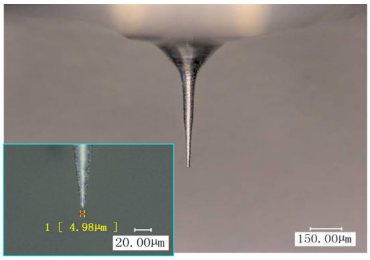

(a) Tool tip of ultra small micro-tool's substrates

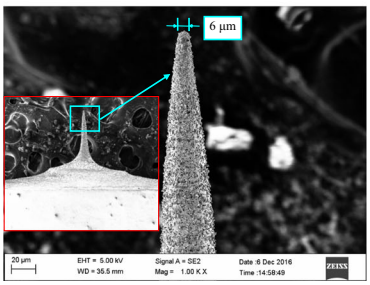

(b) Ultra small micro-grinding tool (d_s=6 μm)

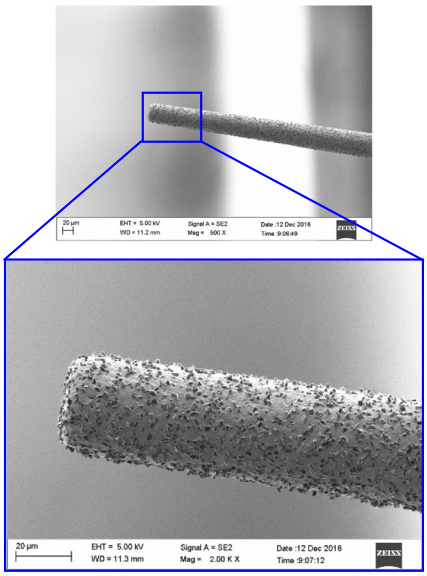

(c) Fabricated diamond micro-grinding tool

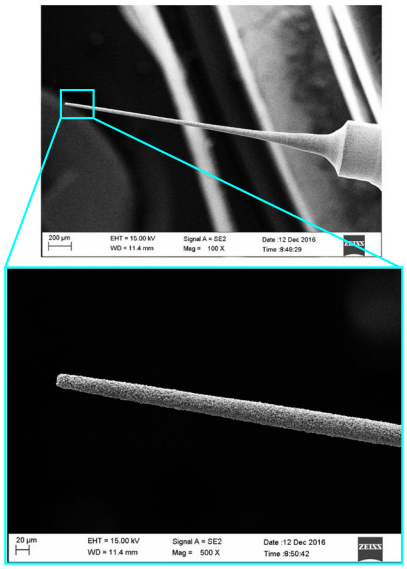

(d) Ultra small micro-grinding tools 1# (d_s<20 μm, L/D ratio>1:50)

Fig. 4 Ultra-small micro-grinding tools fabricated in this study. **a** Tool tip of ultra-small micro-tool substrates. **b** Ultra-small micro-grinding tool (d_s = 6 μm). **c** Fabricated diamond micro-grinding tool. **d** Ultra-small micro-grinding tool no. 1 (d_s < 20 μm, L/D ratio > 1:50)

is directly ground to the final required shape by a grinding wheel with an inclined angle. Then, the machined substrate is electroplated with a controlled motion. Through these two setups, the machining of micro-tool substrate and electroplating process could have low time cost.

The traditional method for fabricating a micro-grinding tool always costs at least 15 min, so of course, it is inefficient. However, using the method of this study, the total time cost for single tool fabrication is within 5 min, which is much lower than those two methods mentioned above.

The substrate of ultra-small micro-grinding tool is ground by an incline plane of grinding wheel. The locating point and the value of inclined angle (θ) are pre-set, and the distance of tool tip (l_t) and tool radius (r_c) could be measured.

$$e_c = 2(r_c - r_o) \tag{1}$$

Equation (1) is the expression of tool diameter error, where e_c is the tool diameter error at a position, r_c is the tool radius at a position, and r_o is the radius of tool tip. For the whole ultra-small micro-grinding tool, it could be deduced by the following equation:

$$e_t = al_t^2 + bl_t + c \quad \left(\theta = 0^\circ, 1^\circ, 2^\circ\right) \tag{2}$$

where e_t is the tool diameter errors along axis direction. In this study, three inclined angle (θ) values are considered at first step (0°, 1°, and 2°). a, b, and c are fitting coefficients. Through these mechanism modeling and experimental result validation, the relationship between tool shape and parameters could be deduced by amounts of experimental results. Finally, the tool's final shape and diameter could be achieved by only one grinding process, from 500 μm to less than 50 μm, which has obvious superiority in time consumption during the ultra-small micro-grinding tool fabrication process.

2.2 Electroplating process

In micro-scale, especially in ultra-small micro-scale, the electroplating process of diamond grains is difficult and critical for the fabrication of micro-grinding tool in this study, and the electroplating process is shown in Fig. 2a. The detailed moving and rotation velocity is controlled previously. The Ni^{2+} ions come from a Ni anode plate and conveyed to the surface of ultra-small micro-grinding substrate. At the same time of metal deposition, the diamond grits are coated. The final diameter of ultra-small micro-grinding tool is determined by the electroplating time. Because of the ultra-small dimension, the influences from chemical effect and micro-scale effect are important and difficult to control. However, only through all of those the diamond grains could be successfully electroplated to the surface of the micro-tool substrate.

When the parameter is not suitable, the electroplating result could be in the situation that Fig. 2b shows. The point discharge effect would significantly influence the diameter of the micro-tool. The d_{e1} and d_{e2} are the tool diameters under the point discharge effect compared with the normal tool diameter (d_0, d_1, and d_2). The electroplating layer thickness of ultra-small micro-grinding tool could be calculated by Eq. (3) and is shown by the following equation:

$$\delta_t = K \cdot D_k \cdot t \cdot \eta_k \cdot \eta_{ds} \tag{3}$$

where δ_t is the electroplating thickness, K is the thickness coefficient, D_k is the cathode-current density, t is the

Table 1 Electroplating solution formula and electroplating technological parameters

Items	Value
Nickel sulfate (g/L)	220
Nickel chloride (g/L)	41
Boracic acid (g/L)	42
Saccharin (g/L)	0.5
Butynediol (g/L)	0.25
Cobaltous sulfate (g/L)	5
Sodium dodecyl sulfonate (g/L)	0.08
Temperature of electroplating solution (°C)	40–45
PH of electroplating solution	4.4–4.9
Abrasive size	W1
Water	Deionized water

electroplating time, η_k is the cathodic current efficiency, and η_{ds} is the ultra-small diameter efficiency, which could be expressed by the following equation:

$$\eta_{ds} = (d_s)^m \cdot 100\% \tag{4}$$

where the d_s is the tool diameter and m is the power exponent which could finally be decided by experiments. After ultra-small micro-grinding tool is successfully fabricated, the electroplating thickness value (δ_{mt}) could be measured by a microscope and the expression of δ_{mt} is shown in the following equation:

$$\delta_{mt} = 0.5(d_n - d_0) \tag{5}$$

where d_n is the diameter value after electroplating for n minutes, and the electroplating thickness value of point discharge effect (δ_{tp}) also could be expressed by the following equation:

$$\delta_{tp} = 0.5(d_{en} - d_0) \tag{6}$$

where d_{en} is the diameter value of the point discharge effect after electroplating for n minutes. The depositing speed of point discharge effect (v_{tp}) could be expressed by the following equation:

$$v_{tp} = \left(\delta_{tp(n)} - \delta_{tp(n-1)}\right)/t \tag{7}$$

where $\delta_{tp(n)}$ and $\delta_{tp(n-1)}$ is the electroplating thickness of the point discharge effect at n minutes and $n-1$ minutes. In order to investigate the effect of tool diameter on electroplating in ultra-small micro-scale, this study has fabricated a lot of ultra-small micro-grinding tools with different tool diameters, from 5 to 120 μm. And, all these fabrication results are equivalent to 0.5 A/dm^2 and 300 s, and the equivalent electroplating thickness (δ_{me}) could be expressed by the following equation:

$$\delta_{me} = \frac{(0.5 \times 300)\delta_{mt}}{D_k \cdot t} \tag{8}$$

Table 2 Micro-grinding experimental parameters

Factors	Value
Diameter of tool (d_s, μm)	30
Micro-slot grinding depth (a_p, μm)	6, 12, 20
Spindle rotation speed (n_g, r/min)	30,000
Feeding speed (v_f, μm/s)	20, 40, 100, 200, 300, 400, 500, 600

3 Experimental setup

3.1 Equipment and fabricated tool

In this study, the micro-tool substrate is fabricated by a grinding wheel, and micro-tools are under monitoring using an endoscope; the tool substrate has a small inclined angle with the diamond grinding wheel. The material of tool substrate is tungsten carbide. Except the grinding equipment for tool substrate machining, an electroplating system has been built for the electroplating process in this study and is shown in Fig. 3a. This system includes equipment such as air supplier, heating unit, DC power, container, and air adjustments. Before the fabrication of ultra-small micro-grinding tool, the electroplating liquid must be heated and mixed first. The resolution and error of the DC power are 10 mV and 1 mA, respectively. Meanwhile, the measuring method of the thickness of electroplated layer is carried out on a high-precision microscope. After the fabrication of ultra-small micro-grinding tool, the final experimental validation process is carried out on a precision machining tool, and the real condition of experiment is shown in Fig. 3b; the material of workpiece is single crystal silicon. This precision micro-machining tool consists of a micro-machining desktop and a digital control system, two vacuum chucks, a coolant system, and so on. Its position resolution is 0.1 μm and has a feed rate working range from 0 to 12.6 m/s.

Figure 4 shows the successfully fabricated micro-tool substrates and electroplated tools, which are made by the method of this study. Different shapes and different dimensions of tool tip are machined. In Fig. 4a, it could be seen that the smallest diameter of substrate is 4.98 μm. Figure 4b shows the smallest micro-grinding tool fabricated in this study, and the diameter of the tool tip is about 6 μm, which is even near the limitation. However, what must be pointed out is that the shape of the tool would has a little cone angle in this small scale (< 6 μm). It is

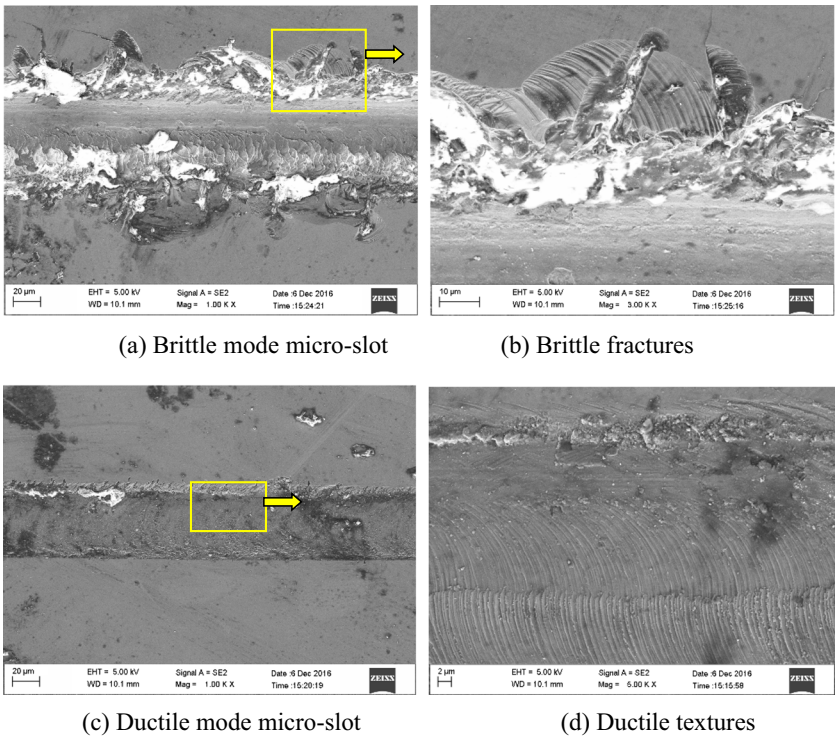

(a) Brittle mode micro-slot (b) Brittle fractures

(c) Ductile mode micro-slot (d) Ductile textures

Fig. 5 Micro-grinding results by ultra-small micro-grinding tool. **a** Brittle mode micro-slot. **b** Brittle fractures. **c** Ductile mode micro-slot. **d** Ductile textures

difficult to maintain the shape precision under this scale because of the material strength of micro-tool itself.

This study has successfully fabricated different kinds of diamond ultra-small micro-grinding tools. Figure 4c shows

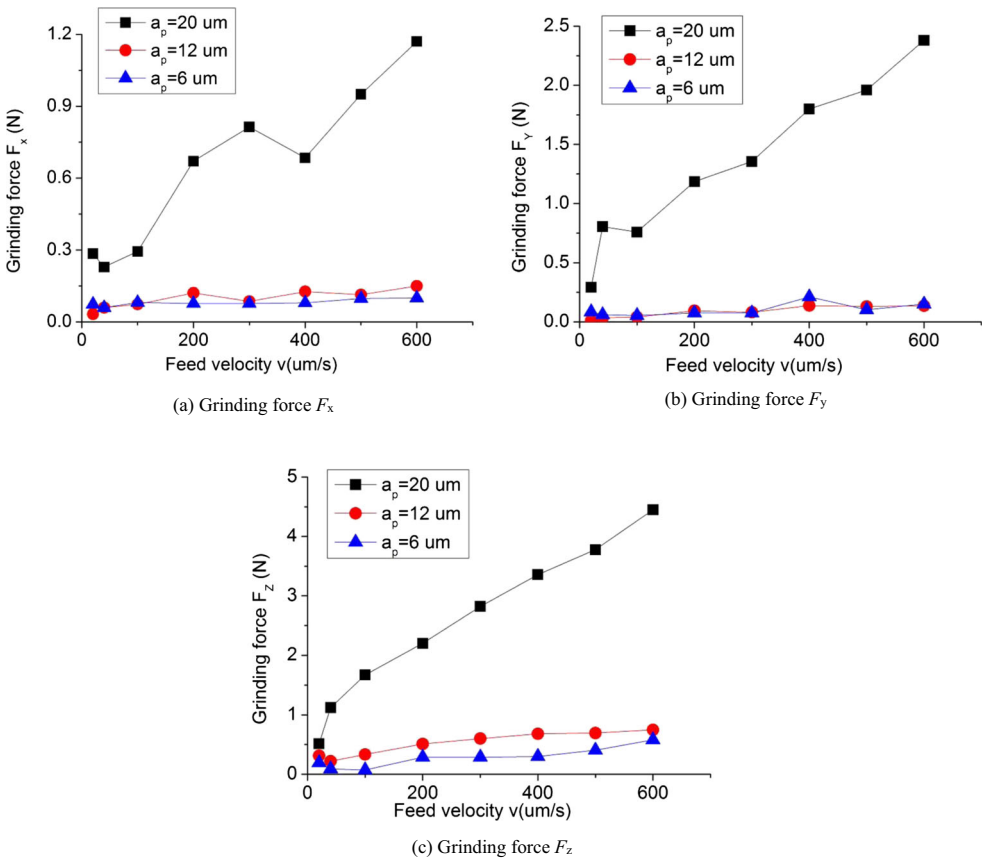

(a) Grinding force F_x

(b) Grinding force F_y

(c) Grinding force F_z

Fig. 6 Grinding forces of ultra-small micro-grinding tool. **a** Grinding force (F_x). **b** Grinding force (F_y). **c** Grinding force (F_z)

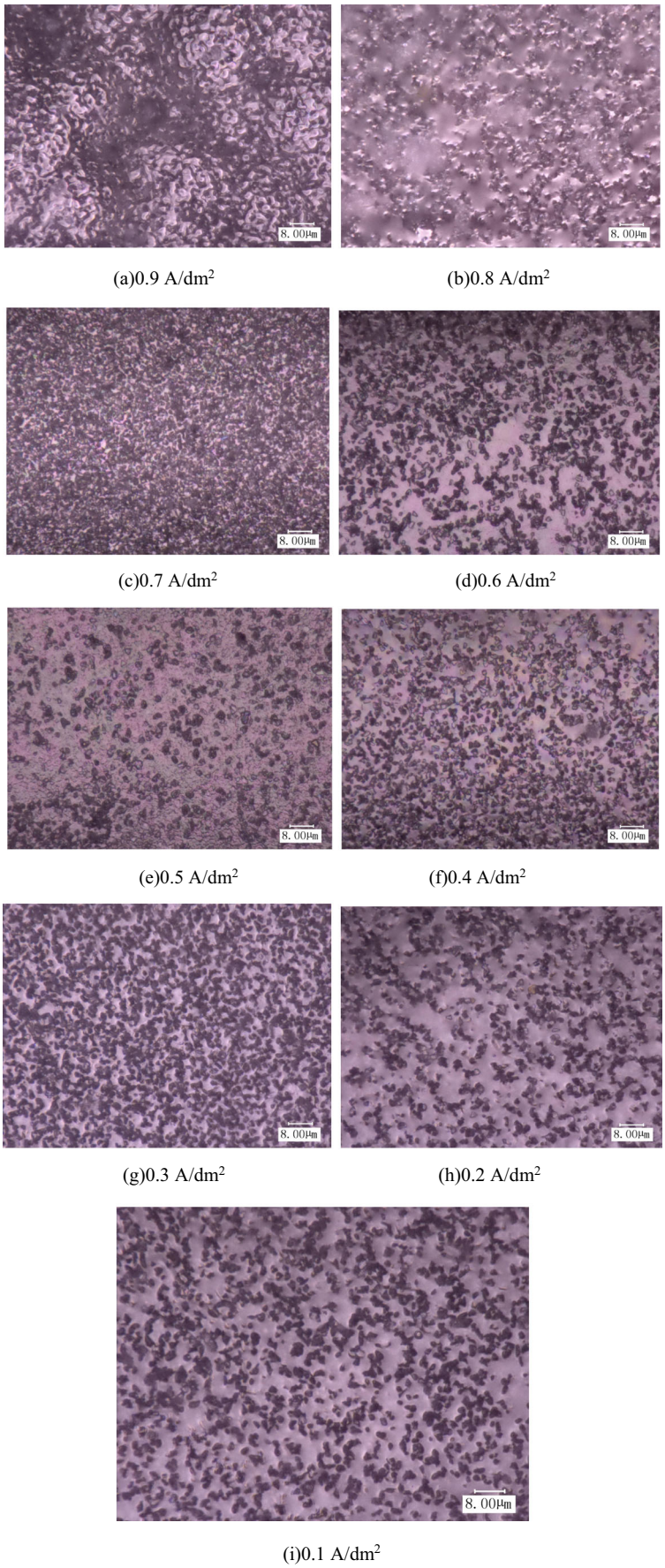

(a)0.9 A/dm^2 (b)0.8 A/dm^2

(c)0.7 A/dm^2 (d)0.6 A/dm^2

(e)0.5 A/dm^2 (f)0.4 A/dm^2

(g)0.3 A/dm^2 (h)0.2 A/dm^2

(i)0.1 A/dm^2

Fig. 7 Electroplating results by different current densities. **a** 0.9 A/dm^2. **b** 0.8 A/dm^2. **c** 0.7 A/dm^2. **d** 0.6 A/dm^2. **e** 0.5 A/dm^2. **f** 0.4 A/dm^2. **g** 0.3 A/dm^2. **h** 0.2 A/dm^2. **i** 0.1 A/dm^2

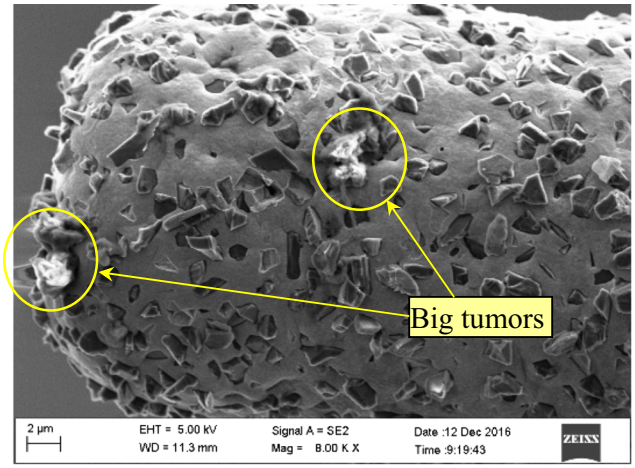

(a) Electroplating tumors

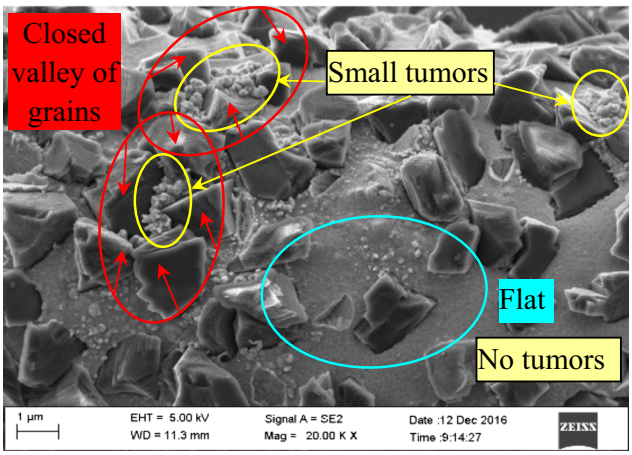

(b) Growing and deposit of small tumors

Fig. 8 Electroplating tumors on the surface of ultra-small-small tool. **a** Electroplating tumors. **b** Growing and deposit of small tumors

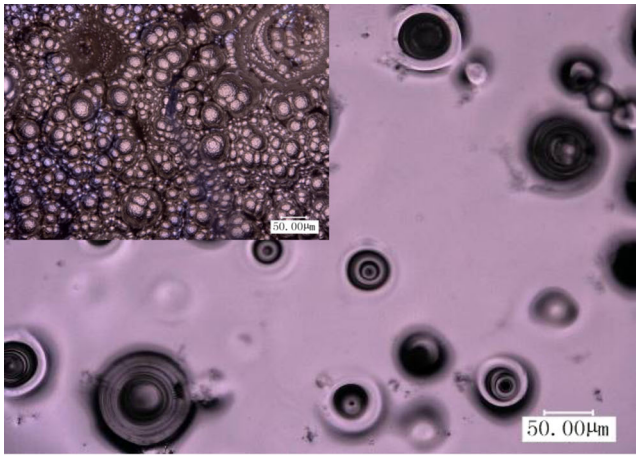

(a) Traditional method

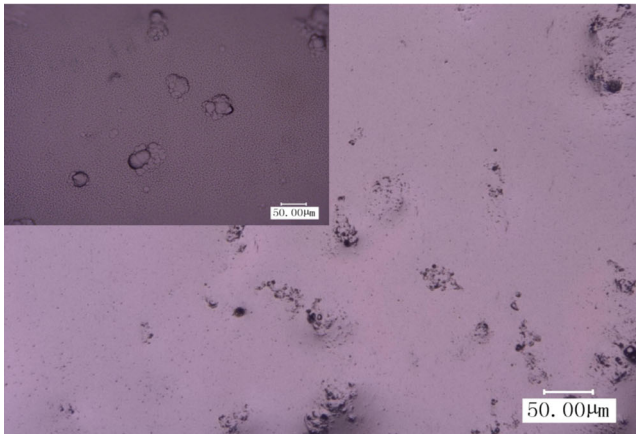

(b) This study method

Fig. 9 The comparison of results of tool surface pre-plating without grains. **a** Traditional method. **b** Method of this study

the ultra-small micro-grinding tool fabricated by the method of this study, and the diameter (d_s) is about 20 μm; it could be seen that the tool fabrication method of this study is applicable. Meanwhile, the size precision and shape precision of ultra-small micro-grinding tool are both well controlled. Figure 4d shows a micro-grinding tool, whose d_s is less than 20 μm and the L/D ratio is larger than 1:50. Things should be specially announced: in this scale, the micro-grinding tool has the largest L/D ratio worldwide until now.

3.2 Design of experiment

After the preparation of 500-μm tool substrate, the next stage is the process of inclined grinding. The grit number of the diamond wheel is 1000, and the diameter of ground micro-tool substrate is less than 50 μm. For all micro-tools that have been fabricated in this study, the substrate material is cobalt-tungsten carbide hard alloy. The inclined angle (θ) is between 0° and 2°. The spindle rotation speed (n_g) is 30,000 r/min, and the feeding speed (v_f) is 200 μm/min.

After the machining of tool substrate, diamond grains should be coated to substrate surface by electroplating process. The electroplating parameters in Eq. (3) are controlled, the cathode-current density (D_k), and the electroplating time (t) are designed to achieve a suitable electroplating thickness (δ_t). Finally, the thickness coefficient (K), the cathodic current efficiency (η_k), and the ultra-small diameter efficiency (η_{ds}) could be revealed by the regression of experimental results. For the electroplating solution formula and electroplating technological parameters, they are listed in Table 1.

Finally, the successfully fabricated tool is employed in a micro-grinding experiment to verify their practical attributes. Table 2 shows the detailed parameters for the experiment. The micro-slot grinding depth (a_p) ranges from 6 to 20 μm. The spindle rotation speed (n_g) is chosen to be 30,000 rpm, which is the most stable condition for the machine tool. The feeding speed (v_f) ranges from 20 to 600 μm/s. Finally, the results of

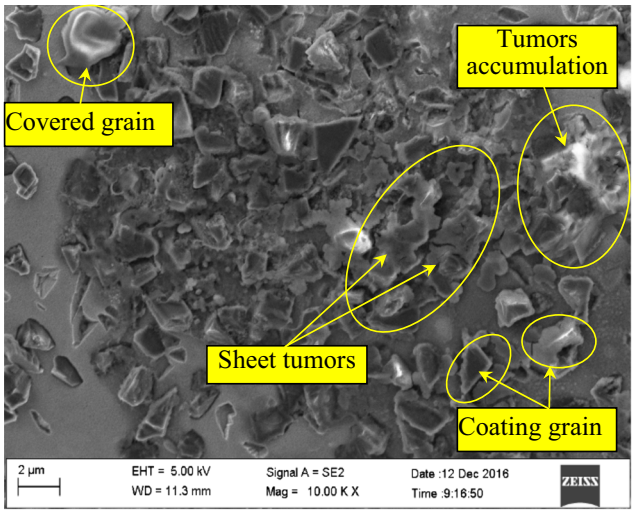

(a) Traditional method

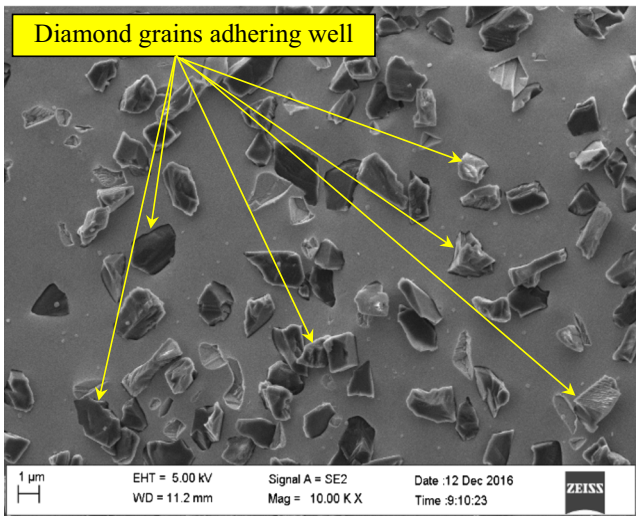

(b) This study's method

Fig. 10 Comparison of electroplating results ($D_k = 0.5$ A/dm^2, $t = 2$ min). **a** Traditional method. **b** Method of this study

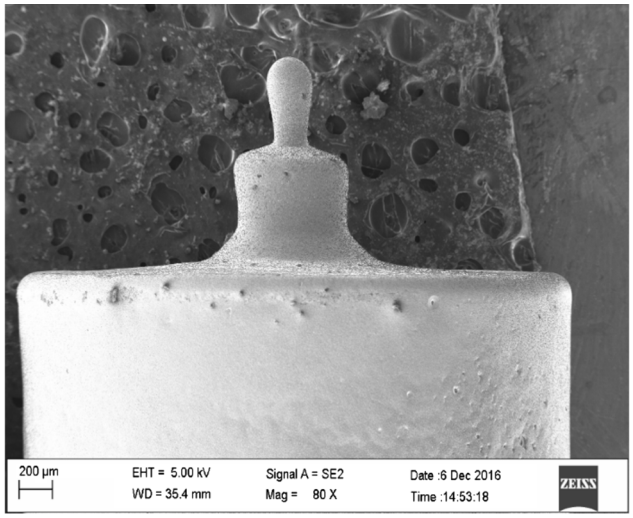

(a) Traditional method

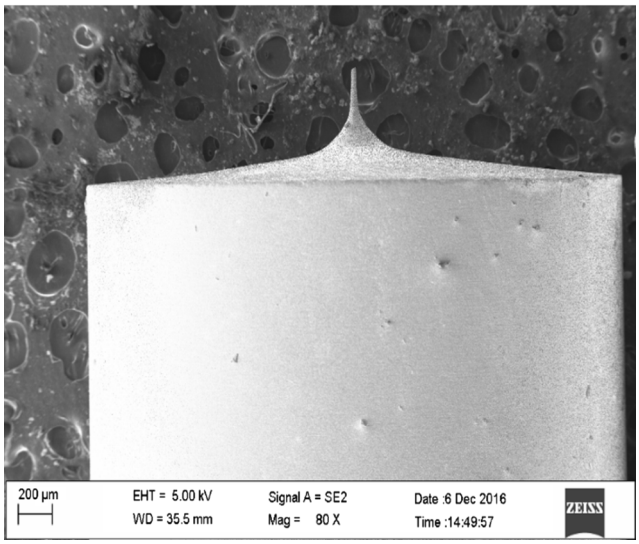

(b) This study's method

Fig. 11 Comparison of final tools between the two methods ($D_k = 0.5$ A/dm^2, $t = 2$ min). **a** Traditional method. **b** Method of this study

experiment, both microscopic images and grinding force data would be analyzed.

3.3 Experimental validation of fabricated tools

In order to verify the practicability of ultra-small micro-grinding tool, which was fabricated in this study, and to investigate the material removal mechanism during the ultra-small micro-grinding process, a series of experiments have been carried out. The brittle-ductile transition is observed, and the grinding force is measured. Figure 5 shows the grinding result created by an ultra-small micro-grinding tool ($d_s = 30$ μm).

Figure 5a is a micro-slot in brittle mode. Based on the detailed observation, it could be found that there are big fractures on its edge, as shown in Fig. 5b. On the contrary, Fig. 5c is a micro-slot in ductile mode. In this mode, it is easy to see the ductile textures on the bottom of micro-slot, which is shown in Fig. 5d.

Based on the investigation above, it clearly shows the procedure from brittle to ductile under different grinding parameters, which also gives a strong proof that the brittle-ductile transition still exists under ultra-small grinding field similar in traditional grinding and normal micro-grinding.

Figure 6 shows the grinding force along three coordinate axes when the grinding depth is 6, 12, and 20 μm, respectively, and it could be seen that the grinding forces increase with the feed velocity (v), which is the same trend as traditional grinding. The deepest ultra-small micro-grinding has the biggest grinding force ($a_p = 20$ μm). The F_z force, along the

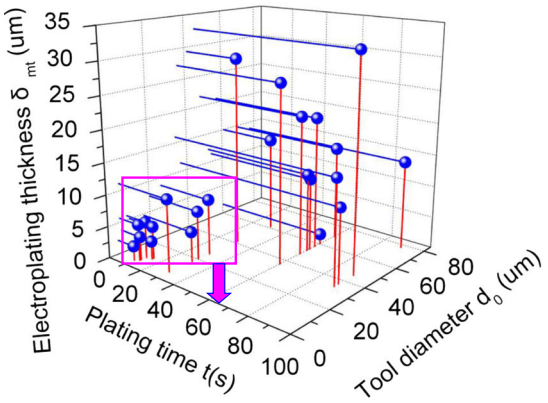

(a) Electroplating thickness δ_{mt} versus plating times and tool diameters

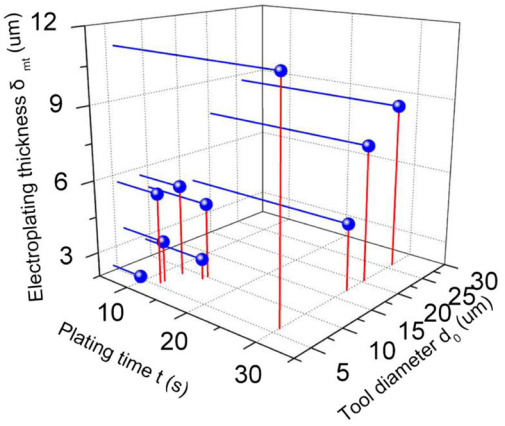

(b) Detailed situation under short plating times and lower tool diameters

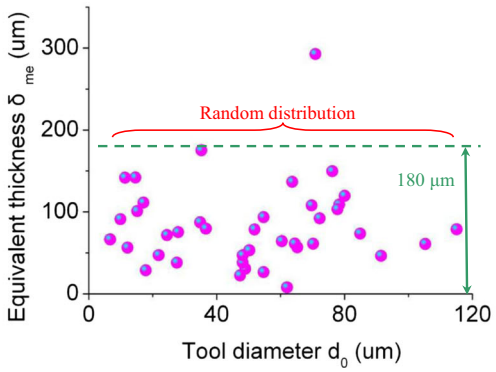

(c) Equivalent thickness δ_{me} versus different tool diameter d_0

Fig. 12 Relationship between electroplating thickness and parameters. **a** Electroplating thickness (δ_{mt}) versus plating times and tool diameters. **b** Detailed situation under short plating times and lower tool diameters. **c** Equivalent thickness (δ_{me}) versus different tool diameters (d_0)

cutting depth direction, is the biggest grinding force in the three directions. The grinding force in the feeding direction (F_y) is a little bigger than the force perpendicular to the feeding direction (F_x). The experiments with smaller dimension are ongoing, and what need to be pointed out is that the force situation is complex when the processing parameter is small during the ultra-small micro-grinding procedure. Lots of influence factors from run-out error and the crystalline effect are induced within this micro-scale range, and this study suggests more investigation should be devoted to this area.

4 Results and discussions

4.1 Electroplating results

In order to investigate the relationship between electroplating results and parameters, the critical condition for the point discharge effect of ultra-small micro-tools should be revealed. This study carried out much electroplating work with different current densities. Figure 7 shows the tool topography and grain distribution situation. It could be seen that the current density (D_k) is an important factor, which could influence the electroplating results significantly. When the D_k value is increased from 0.7 A/dm^2 up to 0.8~0.9 A/dm^2, obvious accumulations and electroplating tumors are observed under a microscope. When D_k decreases from 0.6 to 0.3 A/dm^2, the corresponding electroplating result becomes more stable and uniform. The best result occurs within the range from 0.1 to 0.2 A/dm^2, and in these conditions, diamond grains are well adhered to the surface of substrate and few electroplating tumors appeared on the tool surface. In a word, it would be an effective method to reduce or remove the occurring of electroplating tumors by controlling the value of D_k.

Electroplating tumors shown in Fig. 8a are very harmful in the fabrication of ultra-small micro-tool. For one thing, they break the smooth surface of micro-tool then cause a precision lost. For another, the tumors would induce additional tool wear because of the blocking with chips. The worst of all, they may cause a grinding burn during the grinding process. Figure 8b shows the growing deposit of small tumors on the surface of ultra-small micro-grinding tool in the electroplating

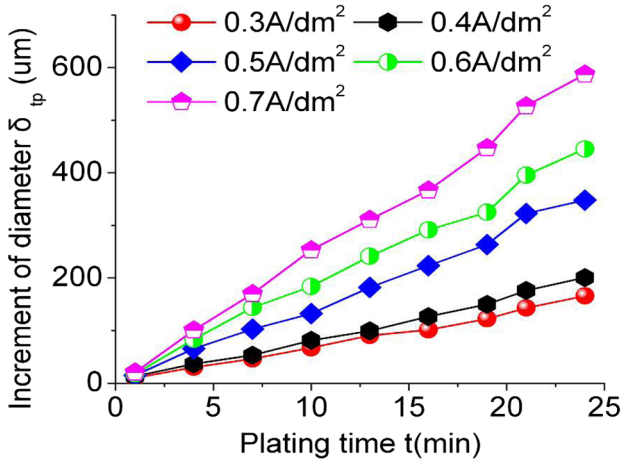

(a) Point effect versus cathode-current density

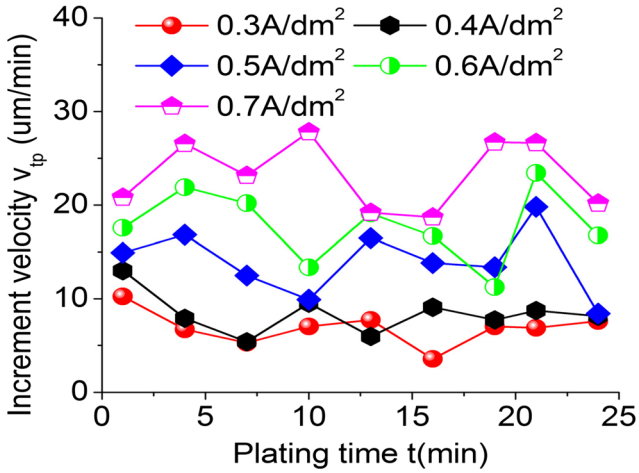

(b) Depositing velocity of point electroplating effect

Fig. 13 Electroplating point discharge effect and its growing velocity in the traditional method. **a** Point effect versus cathode-current density. **b** Depositing velocity of point electroplating effect

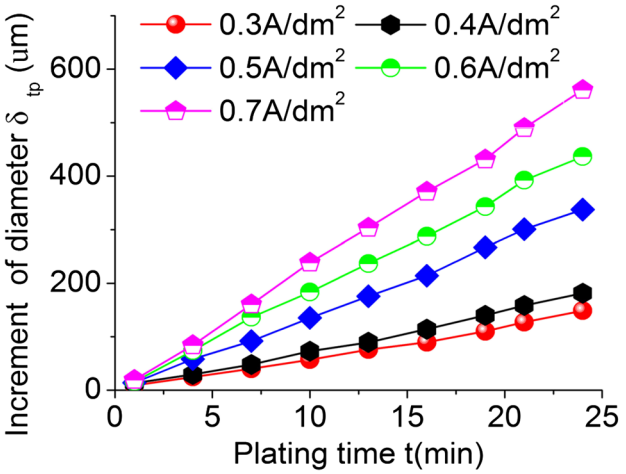

(a) Point effect versus cathode-current density

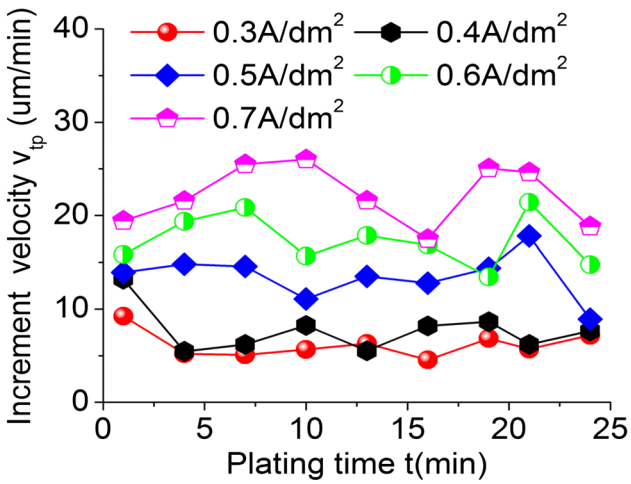

(b) Depositing velocity of point electroplating effect

Fig. 14 Electroplating point discharge effect and its growing velocity by the method of this study. **a** Point effect versus cathode-current density. **b** Depositing velocity of point electroplating effect

process. It could be seen that small tumors easily appeared on a closed valley of diamond grains, and this would cause a comparatively high current in a small area. On contrast, there is no tumor in the area that is flat and without a closed valley. Therefore, it is critical to avoid this phenomenon during the electroplating of ultra-small micro-grinding tool.

4.2 Point discharge and minimization effect

As discussed above, the current density (D_k) is important to the electroplating results, and large D_k could lead to big tumors. Through observation, it is found that this phenomenon always happens in the places of closed grain valley. Therefore, this study develops a novel method to make the electroplated tool to have a continuous motion. By this means, the critical value D_k for the point discharge effect could be increased. The electroplating tumor also is removed under the same parameter. Figure 9 shows the comparison of pre-plating results between two methods. It could be seen that deposit consists bubbles and dusts by traditional method in Fig. 9a, which would cause bad and harmful surface in the formal process. Figure 9b shows the result produced by the method of this study under the same parameter, and it is obvious that this is superior to the result of the traditional method in Fig. 9a.

Under the conditions of a moving substrate or a still substrate, the electroplating results of micro-grinding tool could be significantly different. Figure 10 shows two electroplating results between these two modes when the cathode-current density (D_k) is 0.5 A/dm^2 and the electroplating time (t) is 2 min.

In Fig. 10a, obvious tumors could be found and they keep growing in the traditional method. Figure 10b shows the detailed grain deposition situation of ultra-small micro-grinding

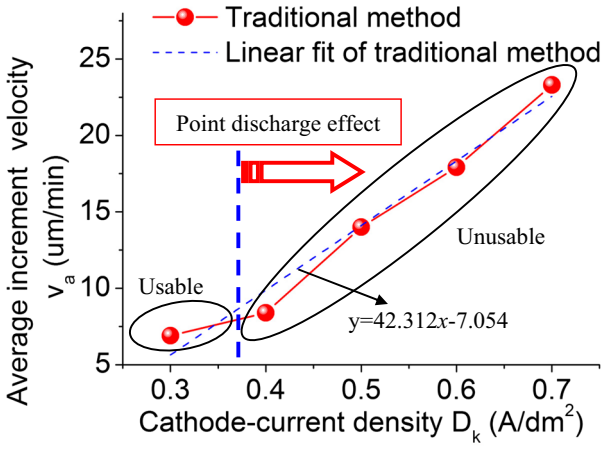

(a) Average increment velocity of traditional method

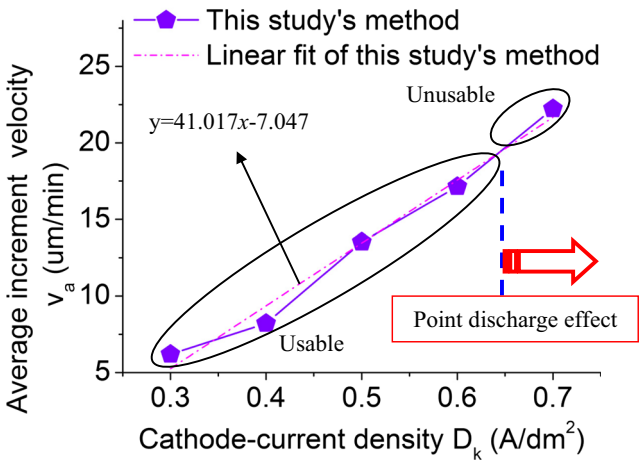

(b) Average increment velocity of this study's method

Fig. 15 Comparison of the average increment velocity between traditional way and the method's way of this study. **a** Average increment velocity of traditional method. **b** Average increment velocity determined by the method of this study

tool fabricated by the method of this study, and the size of grain is 1 μm. It could be seen that the diamond grains are coated to the tool substrate uniformly and without any tumor. Therefore, it is obvious that the study method is superior than the traditional method, and less point discharge phenomenon occurs at the same electroplating parameters.

Finally, this study successfully fabricates several groups of ultra-small micro-grinding tools by both the traditional method and the method of this study, and the tool diameter ranges from 6 to 120 μm. Figure 11 shows the comparison of finally fabricated micro-grinding tools. Figure 11a shows a micro-tool fabricated by the traditional method with an obvious point discharge effect, which causes a big error on both the dimension and the shape of the tool. Figure 11b shows a fabricated ultra-small micro-tool by the method of this study without a point discharge effect. It could be seen that the tool has both well shape and dimension precision.

4.3 Electroplating parameters analysis

For the electroplating process in micro-scale, there are several factors which could influence the result. This study carried out lots of experiments to find the rules and relationship between parameters and fabrication results. Except for the influence of ampere density (D_k), this study also investigates the effect caused by electroplating time (t) and tool diameter (d_0) to the electroplating thickness (δ_{mt}). Figure 12 shows the variation of electroplating thickness with time under different current densities. Figure 12a shows the variation process of δ_{mt}, and the data are all from the fabrication results determined by the method of this study. It could be seen that the electroplating time (t) is the main influence factor to the thickness, and the same rule can be concluded in Fig. 12b when the parameters are low.

In order to investigate the effect of d_0 on δ_{mt}, a calculation is made in this study, which is deduced by Eq. (8) and is shown in Fig. 12c. The electroplating parameters are all equivalent to 0.5 A/dm^2 (D_k) and 300 s (t) to see the effect caused by the factor d_0. The results show that it is different from point discharge effect, and tool diameter (d_0) does not have an obvious regular effect to the electroplating thickness. The equivalent thickness (δ_{me}) has a random distribution from 5 to 180 μm; that is to say, there is no obvious relation between these two factors.

The point discharge effects during the fabrication process are also investigated in this study. Figures 13 and 14 show the measurements of the increment of diameter and its growing velocity in two different ways: traditional way and the method's way of this study, respectively. In traditional way, the increment of diameter (δ_{tp}) caused by a point effect is shown in Fig. 13a, the growing speed is calculated and shown in Fig. 13b, and the above corresponding figure for a new method is shown in Fig. 14a, b, respectively; it should be pointed out that all the results are from real experiments of micro-tool electroplating by this study.

It could be concluded from Figs. 13a and 14a that the increment of diameter (δ_{tp}) increases with the plating time and especially with the increasing of the cathode-current density (D_k). The relationship between plating time (t) and the increment of diameter (δ_{tp}) is near linear. According to Figs. 13b and 14b, it can be seen that the depositing speed of point discharge effect (v_{tp}) is influenced mainly by the cathode-current density (D_k). In addition, it is evident that the data in Fig. 14 are more linear and steady than those in Fig. 13, which also means the superior attribute of the new method of this study.

Except the increment velocity, every single point time is compared, and the average increment velocity in every cathode-current density is also compared based on experimental results. As shown in Fig. 15, it is obvious that the average increment velocity is almost the linear

relationship with the cathode-current density in both the traditional way and the method's way of this study. It could be seen that the influence caused by point discharge effect on the traditional method is more severe than that on the new method, and the point discharge effect occurs when the ampere density (D_k) is about 0.3 A/dm^2 in the traditional method from Fig. 15a. Actually, this is a lower threshold and, undoubtedly, will finally lead to a lower productivity of micro-grinding tool. Figure 15b shows the average increment velocity of the new method of this study, and it could be seen that the occurrence D_k of point discharge effect is delayed to above 0.6 A/dm^2; it is almost twice higher than the traditional method in Fig. 15a.

Obviously, the new method of this study provides a more wide range of the chosen cathode current. Therefore, this superior attribute provided by the method of this study could significantly propel the fabricating technology of the diamond micro-grinding tool.

5 Conclusions

In this study, a new method to fabricate diamond ultra-small micro-grinding tool is presented, and the machining mechanism and its formula expression are given. The electroplating process model in considering the electroplating thickness value of point discharge effect (δ_{tp}) and its depositing speed (v_{tp}) is developed. A series of ultra-small micro-grinding tools, whose diameters are from 6 to 120 μm, have been fabricated by this method. A group of micro-grinding tests on single crystal silicon has been carried out, and the practicality and high productivity of the method of this study are successfully validated. The comparison between this new method and traditional method has been made, and the key findings can be summarized as follows:

(1) A new method for fabricating diamond ultra-small micro-grinding tool is proposed, during which the inclined angle (θ) and the electroplating thickness value (δ_{tp}) of point discharge effect are considered. A series of verification experiments proved that the method of this study has a significant improvement when compared with the traditional method.
(2) The growing small tumors on the surface of ultra-small-small micro-grinding tool in the electroplating process are found. A closed valley of diamond grains would cause a comparatively high current in small area and easily lead to the deposit of tumors.
(3) In the electroplating process using the method of this study, the relationship between plating time (t) and the increment of diameter (δ_{tp}) is near linear. The depositing speed of point discharge effect (v_{tp}) is influenced mainly by the cathode-current density (D_k).
(4) By using the method of this study, the critical D_k value for the occurrence of point effect is delayed to above 0.6 A/dm^2 from about 0.3 A/dm^2 in the traditional method. The effect of tool diameter (d_0) to δ_{mt} is found to be irregular based on a comparison of the equivalent thickness (δ_{me}).

Funding information This paper work is supported by the National Natural Science Fund of China (No. 51575096). The authors would like to thank the support of Shenzhen Changxing Technology Co., Ltd., China.

References

1. Smith PB, Axinte D, Daine M (2015) A study of an improved cutting mechanism of composite materials using novel design of diamond micro-core drills. Int J Mach Tools Manuf 88:175–183
2. Masuzawa T (2000) State of the art of micromachining. CIRP Ann 49(2):473–488
3. Dornfeld D, Min S, Takeuchi Y (2006) Recent advances in mechanical micromachining. CIRP Ann 55(2):745–768.0
4. Smith PB, Axinte D (2012) Solid diamond micro-grinding tools: from innovative design and fabrication to preliminary performance evaluation in Ti-6Al-4V. Int J Mach Tools Manuf 59:55–64
5. Morgan CJ, Vallance RR, Marsh ER (2006) Micro-machining and micro-grinding with tools fabricated by micro electro-discharge machining. Int J Nanomanuf 1(2):242–258
6. Chen ST, Tsai MY, Lai YC (2009) Development of a micro diamond grinding tool by compound process. J Mater Process Technol 209(10):4698–4703
7. Chen ST, Jiang ZH, Wu YY, Yang HY (2011) Development of a grinding-drilling technique for holing optical grade glass. Int J Mach Tools Manuf 51:95–103
8. Cheng J, Yin GQ, Wen Q (2015) Study on grinding force modelling and ductile regime propelling technology in micro drill-grinding of hard-brittle materials. J Mater Process Technol 223:150–163
9. Cheng J, Gong YD (2014) Experimental study of surface generation and force modeling in micro-grinding of single crystal silicon considering crystallographic effects. Int J Mach Tools Manuf 77:1–15
10. Denkena B, Friemuth T, Reichstein M, Tönshoff HK (2003) Potentials of different process kinematics in micro grinding. CIRP Ann–Manuf Technol 51(1):463–466
11. Feng J, Kim BS, Shih A, Ni J (2009) Tool wear monitoring for micro-end grinding of ceramic materials. J Mater Process Technol 209(11):5110–5116
12. Park HW, Liang SY (2008) Force modeling of micro-grinding incorporating crystallographic effects. Int J of Mach Tools Manuf 48(15):1658–1667
13. Lee PH, Lee SW (2011) Experimental characterization of micro-grinding process using compressed chilly air. Int J Mach Tools Manuf 51:201–209
14. Cheng J, Wu J, Gong YD (2017) Grinding forces in micro slot-grinding (MSG) of single crystal sapphire. Int J of Mach Tools Manuf 112:7–20
15. Chen ST, Lai YC (2012) Development of micro co-axial diamond wheel-tool array using a hybrid process of electrochemical co-

deposition and RWEDM technique. J Mater Process Technol 212: 2305–2314
16. Aurich JC, Engmann J, Schueler GM, Haberland R (2009) Microgrinding tool for manufacture of complex structures in brittle materials. CIRP Ann-Manuf Technol 58:311–314
17. Ohmori H, Katahira K, Naruse T (2007) Microscopic grinding effects on fabrication of ultra-fine micro tools. CIRP Ann.-Manuf. Technol 56:569–572
18. Zhu YJ, Ding WF, Huang X, Su HH, Huang GQ (2017) Understanding the residual stress distribution in brazed polycrystalline CBN abrasive grains. Int J Adv Manuf Technol 88:97–106
19. Xu W, Ding WF, Zhu YJ, Huang X, Fu YC (2017) Understanding the temperature distribution and influencing factors during high-frequency induction brazing of CBN super-abrasive grains. Int J Adv Manuf Technol 88:1075–1087